Journal of Solid State Chemistry 182 (2009) 1193–1199

Contents lists available at ScienceDirect

Journal of Solid State Chemistry

journal homepage: www.elsevier.com/locate/jssc

Thermal, solution and reductive decomposition of Cu–Al layered double hydroxides into oxide products

Sylvia Britto, P. Vishnu Kamath *

Department of Chemistry, Central College, Bangalore University, Bangalore 560 001, India

ARTICLE INFO

Article history:
Received 7 November 2008
Received in revised form
16 January 2009
Accepted 1 February 2009
Available online 12 February 2009

Keywords:
Layered double hydroxide
Solution decomposition

ABSTRACT

Cu–Al layered double hydroxides (LDHs) with [Cu]/[Al] ratio 2 adopt a structure with monoclinic symmetry while that with the ratio 0.25 adopt a structure with orthorhombic symmetry. The poor thermodynamic stability of the Cu–Al LDHs is due in part to the low enthalpies of formation of $Cu(OH)_2$ and $CuCO_3$ and in part to the higher solubility of the LDH. Consequently, the Cu–Al LDH can be decomposed thermally (150 °C), hydrothermally (150 °C) and reductively (ascorbic acid, ambient temperature) to yield a variety of oxide products. Thermal decomposition at low (400 °C) temperature yields an X-ray amorphous residue, which reconstructs back to the LDH on soaking in water or standing in the ambient. Solution decomposition under hydrothermal conditions yields tenorite at 150 °C itself. Reductive decomposition yields a composite of Cu_2O and $Al(OH)_3$, which on alkali-leaching of the latter, leads to the formation of fine particles of Cu_2O (<1 μm).

1. Introduction

Layered double hydroxides (LDHs) are derived either from the structure of mineral brucite $[Mg(OH)_2]$, or from that of gibbsite/bayerite $[Al(OH)_3]$ [1], the material obtained in the latter case being Al-rich. Brucite comprises a close packing of hydroxyl ions, in which alternative layers of octahedral sites are occupied by divalent ions, yielding charge-neutral layers having the composition $[M(OH)_2]$ (M^{II} = Mg, Ca, Mn, Fe, Co, Ni). Isomorphous substitution of a fraction of the divalent ions by trivalent ions M' (III) (M' = Al, Cr, Fe, Ga, In) results in layers having the composition $[M(II)_{1-x}M'(III)_x(OH)_2]^{x+}$ ($x \leqslant 0.33$). The positive charge on the layers is compensated by the incorporation of anions such as CO_3^{2-}, NO_3^-, Cl^- in the interlayer region to yield LDHs having the formula $[M(II)_2M'(III)(OH)_6]Cl \cdot mH_2O$ corresponding to $x = 0.33$. Among the brucite-based LDHs, those containing Cu^{2+} as the divalent ion are unique in that the bivalent hydroxide, $Cu(OH)_2$, has a structure closer to that of lepidocrocite (γ-FeOOH) [2] rather than brucite. The difficulties seen in obtaining phase-pure Cu–Al LDHs may be related to the instability of $Cu(OH)_2$. In recent years, many attempts have been made to synthesize phase-pure Cu–Al LDHs [3–7] and in only a few cases has this been achieved [5]. In most studies, malachite $[Cu_2(OH)_2(CO_3)]$, gibbsite and gehrardtite $[Cu_2(OH)_3(NO_3)]$, were also obtained as impurity phases.

Gibbsite is also a layered hydroxide in which the layers have the composition $[Al_{2/3}\square_{1/3}(OH)_2]$ (□: octahedral vacancy). In gibbsite the layers are stacked in the sequence AB BA AB BA----. Among the gibbsite-based LDHs, the most common are the I–III LDHs with Li^+ occupying the cation vacancies of gibbsite [8,9] leading to the layer composition $[Al_{2/3}Li_{1/3}(OH)_2]^{1/3+}$. These LDHs have the composition $[Al_2Li(OH)_6]Cl \cdot 3H_2O$. Recently, however, O'Hare and co-workers [10] have synthesized a series of II–III LDHs derived from gibbsite having the composition $[Al_2M^{II}_{0.5}(OH)_6]Cl \cdot mH_2O$. Here also the LDH containing Cu was found to contain impurity phases. The synthesis of II–III LDHs based on the gibbsite structure creates the possibility of studying a much wider compositional range ([Cu]/[Al] = 2–0.25) than was possible within the brucite-based systems.

The synthesis of LDHs has most commonly been carried out by one of two routes: (i) through coprecipitation at constant pH [11] or (ii) through an oxide route wherein the oxide of the divalent metal is soaked in a salt solution of the trivalent metal [12,13]. In view of the difficulties seen in obtaining phase-pure Cu–Al LDHs, we attempted their synthesis through both the routes given above. While coprecipitation yields a Cu-rich Cu–Al LDH, the oxide route yields an Al-rich Cu–Al LDH.

The interest in Cu–Al LDH stems from the importance of the oxide products derived from these materials in catalysis [7,14–16]. Cu–Al oxides of the spinel structure are used in the oxidation of phenol from aqueous solution [14]. They have also been used in the selective C-alkylation of phenol with methanol [15] and ternary Cu–Zn–Al mixed oxides derived from LDHs have been used as catalysts for low-temperature methanol synthesis [16].

* Corresponding author.
E-mail address: vishnukamath8@hotmail.com (P. Vishnu Kamath).

0022-4596/$ - see front matter © 2009 Elsevier Inc. All rights reserved.
doi:10.1016/j.jssc.2009.02.003

The oxides derived from these LDHs exhibit a high surface area, basicity and greater resistance to sintering [1].

The thermodynamic stability of the LDH is an important factor guiding its decomposition pathway. There are several approaches to understanding the thermodynamic stability of a LDH [17].

(1) As the LDHs are generally decomposed by heating, thermal stability is obtained from calorimetric measurements of the enthalpy of formation [18].
(2) As the LDHs are obtained by alkali precipitation from a mixed metal salt solution, Johnson and coworkers [19] have measured the solubility product of LDHs and related it to their thermodynamic stability. The amphotericity of Cu–Al LDHs, seriously impacts the stability of the LDH in solution.
(3) In contrast to other LDHs, the Cu–Al LDHs are unique owing to the reducibility of the Cu^{2+} ion. Therefore the stability of the LDH is also dictated by the redox potential of Cu^{2+}.
(4) An electronic structure approach can be envisaged taking into consideration such factors as the octahedral CFSEs of the metal ions and the mode of coordination of the anions. This approach has particular significance to the Cu–Al LDHs due to the Jahn-Teller distortion of the Cu^{2+} ion coordination.

In this paper we report the synthesis and characterization of brucite and gibbsite-based Cu–Al LDHs. We study their breakdown through the thermal, solution and reductive decomposition routes and examine the products obtained from each and their possible applications.

2. Experimental

2.1. Synthesis of Cu_2Al–CO_3 LDH

A mixed metal nitrate solution containing stoichiometric amounts of Cu and Al (2:1) was added drop-wise to a $NaHCO_3$ solution (100 mL) containing four times the stoichiometric excess of carbonate ions. The pH was maintained at 10 using a Metrohm Model 718 STAT Titrino operating in the pH STAT mode. The reaction was carried out at room temperature under vigorous stirring. The blue precipitate was aged in the mother liquor (16 h). It was then washed 3–4 times with deionized Type-II water (Millipore Elix-3 water purification system, specific resistance 15 MΩ cm), once with ethanol and dried in an air oven at 65 °C.

2.2. Synthesis of $CuAl_4$–NO_3 LDH

A 1 g of CuO was made into a slurry in 15 mL of 0.7 M $Al(NO_3)_3$ solution and aged in an air oven at 65 °C for four days. The precipitate was then washed several times with deionized water, once with ethanol and dried in an air oven at 65 °C.

2.3. Hydrothermal and thermal decomposition

Both the Cu_2Al–CO_3 LDH and the $CuAl_4$–NO_3 LDH were hydrothermally treated at temperatures ranging from 110 to 180 °C. In a typical procedure, 0.5 g of LDH was dispersed in 40 mL of deionized water (50% filling) and hydrothermally treated in a Teflon-lined autoclave at the required temperature for 24 h. We refer to the decomposition of the LDH under hydrothermal treatment as solution decomposition. In separate experiments, the LDHs were also calcined in a muffle furnace at 400, 600 and 800 °C for 18 h each.

2.4. Reversible thermal behavior

A 0.5 g batches of the LDHs were calcined at 400 °C for 4 h in a muffle furnace. Complete decomposition is indicated by the mass loss. In separate experiments, the amorphous residue was stirred for two days in a Na_2CO_3 solution or equilibrated in a water-saturated environment. The product was collected in a previously weighed sintered glass crucible and the mass gain monitored.

2.5. Reductive decomposition

Three hundred and seventy milliliter of a solution containing 2.6 g of ascorbic acid was adjusted to pH 10 using 1 M NaOH. To this solution, 2 g of the $CuAl_4$-LDH was added and the suspension stirred at room temperature for 3 h. The yellow product obtained was centrifuged, washed several times with deionized water, twice with ethanol and dried in a dessicator. The resultant product was found to be a composite of Cu_2O–$Al(OH)_3$. One gram of the composite was soaked in 50 mL of 6 M NaOH in a screw capped polypropylene vessel and kept at 65 °C in an air oven for 6 h to leach out the $Al(OH)_3$. The residue was filtered through a previously weighed sintered glass crucible and the mass loss monitored.

2.6. Characterization

Powder diffraction data were collected on a Bruker D8 Advance powder X-ray diffractometer (Cu$K\alpha$ radiation, $\lambda = 1.5418$ Å). Data were collected at a continuous scan rate of $1^\circ\ 2\theta\,\mathrm{min}^{-1}$ and rebinned into steps of $0.02^\circ\ 2\theta$. TG data were obtained using a Mettler Toledo TGA/SDTA Model 851^e system (30–800 °C, heating rate 5 °C min^{-1}, flowing air). IR spectra were obtained using a Nicolet Model Impact 400D FTIR spectrometer (KBr pellets, 4000–400 cm^{-1}, resolution 4 cm^{-1}). Scanning electron micrographs were obtained using a JEOL Model JSM 840 microscope. The powder samples were dispersed on a double sided conducting carbon tape. The samples were sputter coated with gold to improve conductivity.

The Cu and Al content in the LDHs was estimated by gravimetric analysis. Cu was estimated using the benzoin-α-oxime (cupron) method [20]. Aluminium was estimated using 8-hydroxyquinoline as the precipitant [20] after the removal of Cu as CuS.

3. Results

3.1. Synthesis and characterization of Cu_2Al–CO_3 LDH

In Fig. 1(a) is shown the PXRD pattern of the Cu–Al LDH obtained by coprecipitation. All the observed reflections (up to 65° 2θ) are indexed on a monoclinic cell using the cell parameters given by Yamaoka and coworkers [3] ($a = 15.21$ Å, $b = 2.9$ Å, $c = 5.86$ Å, $\beta = 100.3^\circ$) (Table 1). There are no impurities of a crystalline nature. The wet chemical analysis and TGA data (Table 2) yield an approximate formula $[Cu_{0.7}Al_{0.3}(OH)_2](CO_3)_{0.15}\cdot 0.8H_2O$. The basal reflections are sharp while the non-basal reflections ($>30^\circ\ 2\theta$) are considerably broadened. Such non-uniform broadening is due to the presence of stacking faults [21–23]. On hydrothermal treatment at 110 °C for 24 h, the LDH structure is retained and the reflections in the mid-2θ region ($30–50^\circ\ 2\theta$) are distinctly sharper indicating structural ordering (see Fig. 1(b)).

The CO_3^{2-} ion intercalated in the D_{3h} symmetry exhibits three IR active modes corresponding to the out-of-plane bending ν_2

(A_2'': 870 cm^{-1}), antisymmetric stretching v_3 (E': 1360 cm^{-1}) and in-plane bending v_4 (E': 670 cm^{-1}). The IR spectrum of the Cu–Al–CO_3 LDH in the carbonate absorption region (Fig. 2) however shows a splitting of the doubly degenerate v_3 (1362 and 1380 cm^{-1}) and v_4 modes (600 and 640 cm^{-1}) corresponding to the A_1+B_2 modes of C_{2v} symmetry. This combined with activation of the v_1 mode (1025 cm^{-1}) indicates lowering of the carbonate symmetry from D_{3h} to C_{2v} in the Cu–Al–CO_3 LDH. The v_1 mode is more pronounced in the hydrothermally treated sample (data not shown).

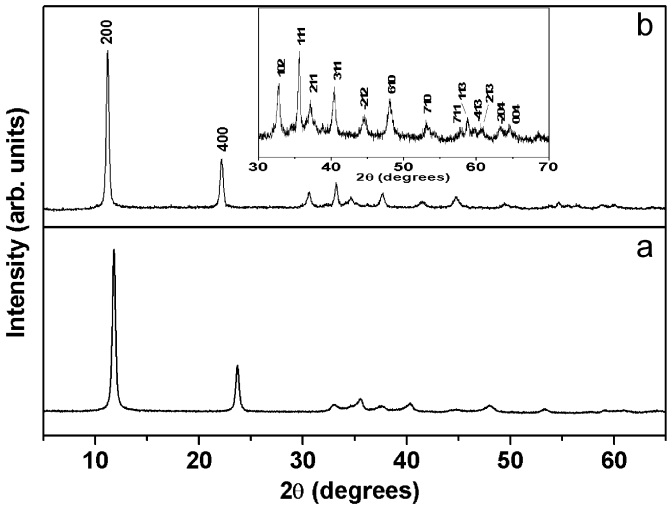

Fig. 1. PXRD patterns of Cu_2Al–CO_3 LDH (a) as prepared and (b) on hydrothermal treatment at 110 °C (inset: 30°–70° 2θ region expanded).

Table 1
Calculated and observed d-spacings of the PXRD patterns of the Cu_2Al–CO_3 LDH and $CuAl_4$–NO_3 LDH.

Cu_2Al–CO_3 LDH (monoclinic cell)			$CuAl_4$–NO_3 LDH (orthorhombic cell)		
d (obs.) (Å)	d (calc.)[a] (Å)	$h\,k\,l$	d (obs.) (Å)	d (calc.)[b] (Å)	$h\,k\,l$
7.481	7.481	200	8.605	8.595	200
3.749	3.741	400	4.285	4.298	400
2.734	2.741	102	3.168	3.176	221
2.520	2.519	111	3.079	3.099	420
2.414	2.389	211	2.511	2.513	112
2.231	2.227	311	2.291	2.279	022
2.032	2.039	−212	2.219	2.224	431
1.891	1.891	610	2.009	2.004	241
1.721	1.721	710	1.481	1.482	523
1.589	1.587	711	1.459	1.459	651
1.569	1.568	113			
1.545	1.559	−413			
1.522	1.521	213			
1.466	1.465	−204			
1.441	1.442	004			

[a] $a = 15.207$ Å, $b = 2.9$ Å, $c = 5.86$ Å, $\beta = 100.3°$.
[b] $a = 17.19$ Å, $b = 8.94$ Å, $c = 5.30$ Å.

Other CO_3^{2-}-containing LDHs crystallize in a three-layered rhombohedral structure and the CO_3^{2-} ions occupy the trigonal prismatic interlayer sites [24]. This structure is preferred to other polytypes as the prismatic site maximizes the H-bonding between the oxygen of the CO_3^{2-} ions and the hydroxyl groups of the metal hydroxide slab [25]. However there are other polytypes, notably those of hexagonal symmetry, that also provide prismatic sites for CO_3^{2-} incorporation [26]. Laboratory prepared samples are therefore obtained as intergrowths of two or more polytypes. The intergrowth regions manifest as regions comprising stacking faults. The stacking faults once incorporated cannot be eliminated by hydrothermal treatment [27]. The Cu–Al system is therefore an exception among the LDHs in that ordering is observed on hydrothermal treatment. Although detailed structure of the Cu–Al LDH is not known, the facile ordering of the LDH is a manifestation of the differences in the structure of this LDH when compared to other LDHs.

(a) In contrast to other II–III LDHs, the Cu–Al LDH crystallizes with monoclinic symmetry.
(b) On monoclinic distortion, the interlayer sites lose three-fold symmetry. The incompatibility between the local symmetry of the interlayer site and symmetry of the CO_3^{2-} ion, destabilizes the stacking disorders whereby partial ordering is observed on hydrothermal treatment. Complete ordering however is preceded by decomposition at 150 °C.

3.2. Synthesis and characterization of $CuAl_4$–NO_3 LDH

In Fig. 3(a) is shown the PXRD pattern of the product obtained by soaking CuO in $Al(NO_3)_3$ solution. The pattern is indexed to an

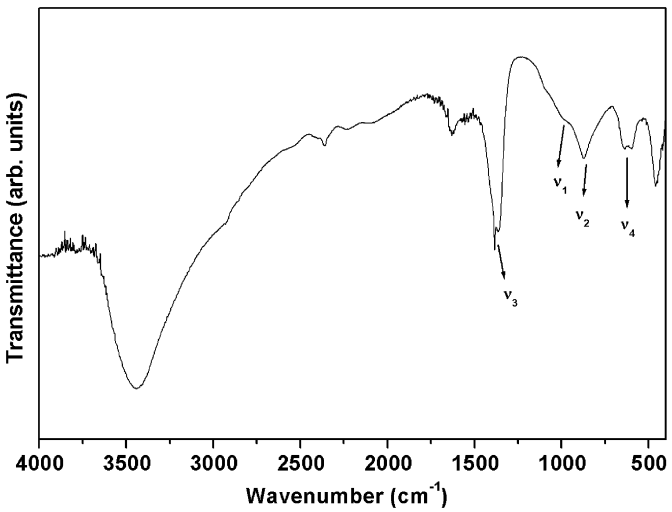

Fig. 2. Infrared spectrum of the Cu_2Al–CO_3 LDH.

Table 2
Elemental analysis and TGA mass loss data of the Cu_2Al–CO_3 LDH and $CuAl_4$–NO_3 LDH.

Sample	Cu/Al ratio	% Mass loss from TGA	Approximate formula[a]
Cu_2Al–CO_3 LDH	2.3	35.7	$Cu_{0.7}Al_{0.3}(OH)_2(CO_3)_{0.15}\cdot 0.8H_2O$
$CuAl_4$–NO_3 LDH	0.24	47.7	$Cu_{0.17}Al_{0.67}(OH)_2(NO_3)_{0.33}\cdot 0.35H_2O$

[a] Computed on the basis of Cu/Al ratio and water content calculated from TGA mass loss.

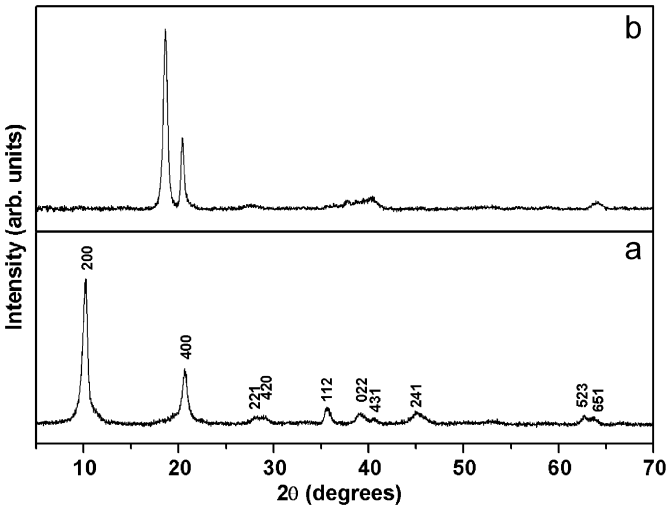

Fig. 3. PXRD patterns of $CuAl_4$–NO_3 LDH (a) as-prepared and (b) after hydrothermal treatment (120 °C).

orthorhombic cell ($a = 17.19$ Å, $b = 8.94$ Å, $c = 5.29$ Å) (see Table 1). Wet chemical analysis yields an approximate formula $[Cu_{0.17}Al_{0.67}(OH)_2](NO_3)_{0.33} \cdot 0.35H_2O$ (see Table 2). This structure is reported to be closely related to the gibbsite-based Li–Al LDHs except that only half the octahedral vacancies in gibbsite are occupied by Cu^{2+} [10]. Gibbsite-based Li–Al LDH is prepared by an 'imbibition' reaction in which the Li^+ ions are topotactically inserted into the $[\square_{1/3}Al_{2/3}(OH)_2]$ (□: cation vacancy) slab through the triangular faces of the $[\square(OH)_6]$ octahedra by a mechanism called diadochy [28]. Insertion of divalent ions into gibbsite is however not facile and requires harsh conditions [10]. We are able to synthesize the Cu–Al_4 LDH by a simpler route involving soaking of CuO in $Al(NO_3)_3$ solution. Fig. 3(b) shows the PXRD pattern of the product obtained upon hydrothermal treatment of $CuAl_4$–NO_3 LDH (120 °C, 24 h). The LDH has decomposed leaving behind $Al(OH)_3$. The absence of any peaks due to CuO and the blue color of the supernatant indicates the deintercalation of Cu^{2+} ions. An estimation of Cu content in the supernatant confirms leaching out of copper from the LDH (Obs.: 9.4%; Exp.: 11.7%).

3.3. Thermal behavior

The TGA curve of the Cu_2Al-LDH is shown in Fig. 4(a). The LDH loses mass in two steps. The lower temperature mass loss is observed from 30 to 550 °C and a higher temperature mass loss is seen from 550 to 800 °C. The DTG curve shows that the LDH decomposes at 150 °C. The total mass loss (35.7%) over the 30–800 °C range is consistent with the following reactions:

$$[Cu_{0.7}Al_{0.3}(OH)_2](CO_3)_{0.15} \cdot 0.8H_2O \rightarrow 0.15\ CuAl_2O_4 + 0.55\ CuO$$

In contrast, the TGA curve of the $CuAl_4$–NO_3 LDH (Fig. 4(b)) indicates a single step mass loss with decomposition occurring at 250 °C (the mass loss below 100 °C is attributed to loss of physisorbed water). The mass loss (47.7%) is consistent with the following reaction:

$$[Cu_{0.17}Al_{0.67}(OH)_2](NO_3)_{0.33} \cdot 0.35H_2O \rightarrow 0.165\ CuAl_2O_4 + 0.165\ Al_2O_3$$

In Fig. 5(a) is shown the PXRD pattern of the oxide residue obtained on thermal decomposition (400 °C, 4 h) of the Cu_2Al–LDH. The material is X-ray amorphous. Disappearance of basal reflections in the PXRD pattern and of the CO_3^{2-}-related vibrations in the IR spectrum indicates breakdown of the LDH structure. On soaking the amorphous residue in Na_2CO_3 solution, the LDH is reconstructed (Fig. 5(b)). However, only 79% of the original mass is regained possibly due to partial bulk dissolution. Reconstruction is also observed on equilibrating the oxide residue at the ambient temperature under 100% relative humidity (Fig. 5(c)). In this case 99% recovery of mass was observed. A further evidence of reconstruction is the restoration of CO_3^{2-}-related vibrations in the IR spectrum of the reconstructed samples (data not shown). Decomposition at higher temperatures leads to the formation of the more stable CuO which does not reconstruct. At even higher temperatures (800 °C), $CuAl_2O_4$-related peaks appear in the PXRD pattern (Fig. 6(a)).

In Fig. 7(a) is shown the PXRD pattern of the sample obtained on decomposing $CuAl_4$-LDH at 400 °C. The disappearance of basal reflections indicates breakdown of the LDH structure. The pattern obtained on soaking the residue in Na_2CO_3 solution is shown in Fig. 7(b). The pattern could be indexed to a mixture of Cu_2Al–CO_3

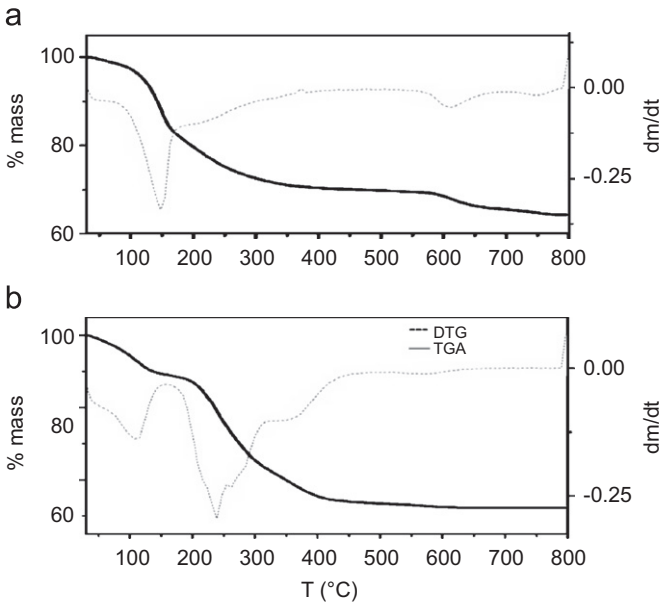

Fig. 4. TGA and DTG curves of the (a) Cu_2Al–CO_3 LDH and (b) $CuAl_4$–NO_3 LDH.

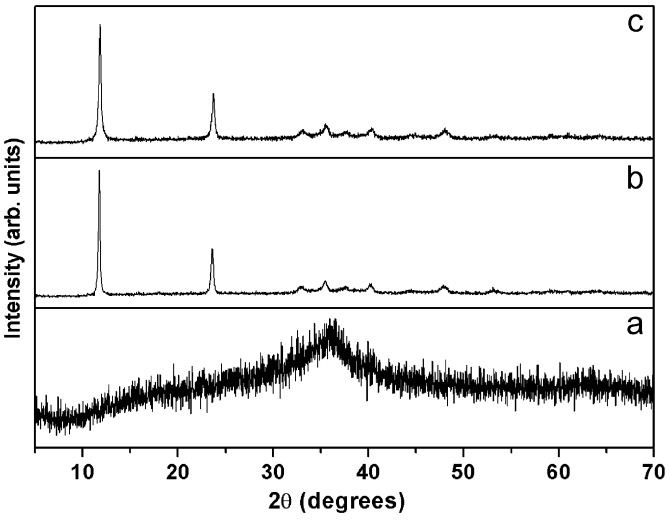

Fig. 5. PXRD pattern of the (a) oxide residue obtained on thermal decomposition (400 °C, 4 h) of the Cu_2Al-LDH, (b) product obtained on soaking (a) in Na_2CO_3 solution, and (c) on equilibrating (a) in a water-saturated atmosphere.

LDH and $Al(OH)_3$. On decomposing the LDH at even higher temperatures (600–800 °C), poorly crystallized $CuAl_2O_4$ is obtained (Fig. 6(b)) which does not reconstruct back to the LDH.

Among the layered hydroxides, the reconstruction phenomenon has been exhibited only by the LDHs of Mg and Zn with Al [29,30]. In these LDHs, Al^{3+} substitutes for some of the Mg^{2+} in the MgO to form a defect oxide having the rocksalt structure. Due to the compositional metastability of this oxide residue, it rapidly reverts back to the LDH structure. The LDHs of Ni and Co, which form spinels at a low temperature, do not exhibit reversible thermal behavior. In the case of the Cu–Al system also, thermal decomposition leads to an X-ray amorphous metastable oxide intermediate of unknown structure. Formation of the stable oxide (tenorite, CuO) and reconstruction to the LDH are competing pathways accessible to the oxide residue. At lower temperatures as formation of LDH from the metastable intermediate is kinetically favored, the intermediate reverts back to the LDH structure by absorption of CO_2 and moisture from the atmosphere. On heating to higher temperatures however, the activation barrier to formation of tenorite is overcome and the metastable intermediate is transformed to the stable tenorite, which being more stable than the LDH, does not reconstruct. In the case of the $CuAl_4$-LDH, the presence of broad peaks at 37° and 45° indicate possible formation of the more stable γ-Al_2O_3. Reconstruction is therefore not observed in humid atmosphere. On soaking in Na_2CO_3 solution however, dissolution of the oxide residue is facilitated and the more stable phases, Cu_2Al–CO_3 LDH and $Al(OH)_3$ are precipitated in preference to $CuAl_4$-LDH.

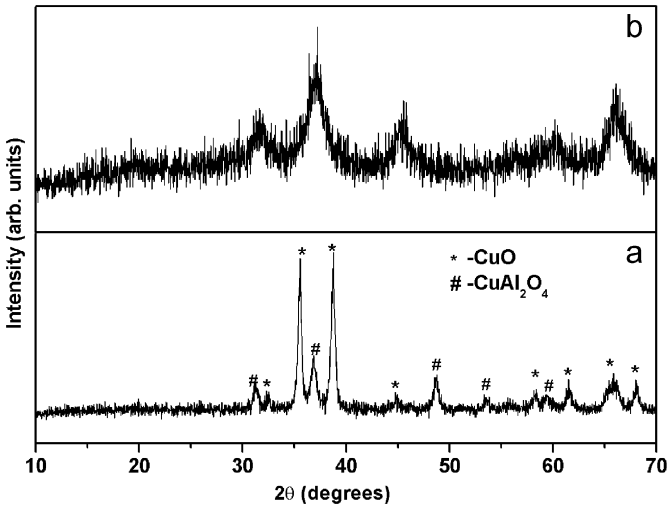

Fig. 6. PXRD pattern of the oxide residue obtained on thermal decomposition (800 °C, 4 h) of the (a) Cu_2Al-LDH and (b) $CuAl_4$-LDH.

3.4. Solution decomposition

As discussed earlier, while hydrothermal treatment at 110 °C leads to structural ordering of the Cu_2Al-LDH, treatment at higher temperatures (150 °C) leads to the formation of crystalline CuO (major phase) and boehmite, AlOOH (minor phase) (Fig. 8(a)). The formation of crystalline CuO at much lower temperatures than during thermal decomposition is related to the fact that under these conditions decomposition proceeds via dissolution and reprecipitation. As explained by Cuddenec and co-workers [31], upon dissolution, the Cu^{2+} ion adopts a square planar coordination in the complex anion $[Cu(OH)_4]^{2-}$. This is a precursor to CuO which also has Cu^{2+} in square planar coordination.

In contrast, under solid state decomposition conditions, formation of tenorite requires rearrangement of the coordination environment of Cu^{2+} from that in the LDH to the square planar environment in tenorite. The kinetic barrier leads to formation of an intermediate metastable amorphous oxide residue below 600 °C before formation of tenorite at higher temperatures.

The $CuAl_4$-LDH also breaks down at lower temperatures under hydrothermal conditions than under thermal conditions. As it is Al^{3+}-rich, it gives rise to boehmite and bayerite (Fig. 8(b)). Cu^{2+} is leached out upon hydrothermal treatment.

3.5. Reductive decomposition

Due to the reducibility of the Cu^{2+} ion, the Cu–Al LDH lattice can also be broken down by reductive decomposition. In Fig. 9(a) is shown the PXRD pattern of the product obtained on the reduction of $CuAl_4$-LDH by ascorbic acid. The pattern indicates a composite of Cu_2O and $Al(OH)_3$. We explore the potential of this material as a precursor to fine particulate Cu_2O. Due to the insolubility of Cu_2O in alkali, $Al(OH)_3$ may be selectively leached out leaving behind fine particles of Cu_2O. This strategy is similar

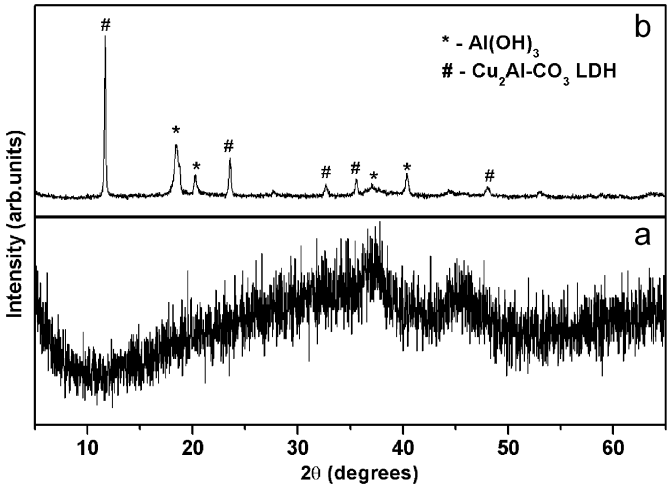

Fig. 7. PXRD pattern of (a) oxide residue obtained on thermal decomposition (400 °C, 4 h) of the $CuAl_4$-LDH and (b) product obtained on soaking (a) in Na_2CO_3 solution.

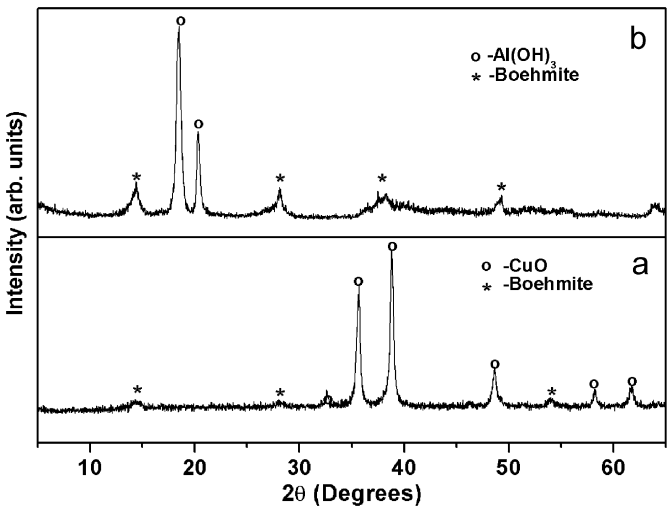

Fig. 8. PXRD pattern of the product obtained on hydrothermal treatment of (a) Cu_2Al–CO_3 LDH and (b) $CuAl_4$–NO_3 LDH at 150 °C.

to that used by other authors [32–34] for the synthesis of macroporous materials. In Fig. 9(b) is shown the PXRD pattern of the residue obtained on soaking the composite in alkali. Selective leaching out of the $Al(OH)_3$ leaves behind single phase Cu_2O. The mass loss obtained on leaching of $Al(OH)_3$ is quantitative. The SEM images of the Cu_2O–$Al(OH)_3$ composite is shown in Fig. 10(a). It is seen to consist of large monolithic particles in the μm range. On leaching of $Al(OH)_3$, the SEM image (Fig. 10(b)) shows smaller sub-micron sized particles.

Attempts were made to synthesize fine particle Cu_2O from the Cu_2Al-LDH precursor. However on reduction of Cu_2Al–CO_3 LDH in ascorbic acid, only Cu_2O peaks are observed (see Fig. 11). The possibility that the $Al(OH)_3$ is present as an amorphous phase is however ruled out by the absence of any mass loss on soaking the product obtained in alkali. This implies that the $Al(OH)_3$ has undergone dissolution during the reduction stage itself.

4. Discussion

There has been a considerable degree of confusion in the early literature regarding the formation of Cu–Al LDHs. It was believed that Cu^{2+} can be incorporated into LDHs only in the presence of another divalent ion [1]. The difficulties associated with the synthesis of Cu–Al LDHs may be related to the lower thermodynamic stability of this LDH. We now look more closely at the stability of the Cu–Al LDH from the point of view of thermochemistry, solubility and electronic structure as has been elucidated in the introduction to this paper.

Navrotsky and co-workers [18] have pointed out that for systems where thermodynamic data are not available, a simple approach to determine the enthalpy and free energy of formation would be to consider the LDH to consist of a mechanical mixture of binary hydroxides and carbonates. Lack of detailed structural information pertaining to Cu–Al LDHs limits the extent to which such an approach may yield accurate thermodynamic values for the Cu–Al LDHs. Nevertheless, a qualitative understanding of the relative stability of the Cu–Al LDHs with respect to other M^{2+}–Al LDHs may be made. This 'mechanical mixture' model shows that a large contribution to the stability of a LDH is derived from the divalent salt of the interlayer anion with a smaller (but not negligible) contribution from the divalent hydroxide. Unlike carbonates of other divalent ions which have the calcite structure, the carbonate of copper is stable as the basic carbonate, malachite. Cupric carbonate ($CuCO_3$) decomposes in a facile way to CuO and CO_2. Furthermore, the free energy of formation of $Cu(OH)_2$ is lower than that of the other divalent hydroxides such as $Mg(OH)_2$ and $Co(OH)_2$ [$\Delta G^0_{298}[Cu(OH)_2] = -85.3\,kcal\,mol^{-1}$,

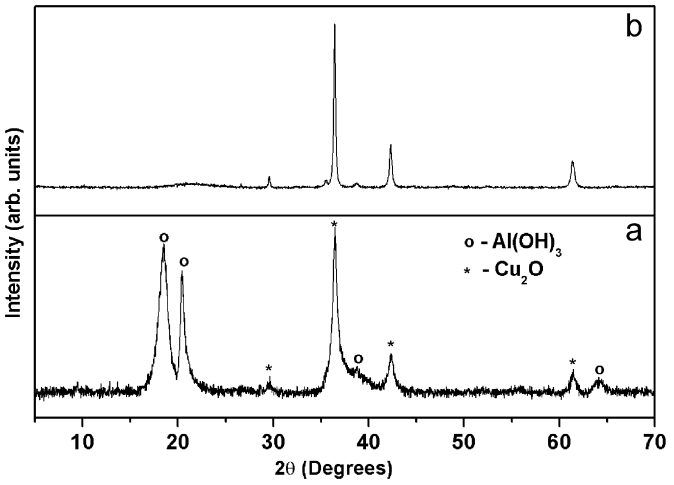

Fig. 9. PXRD pattern of product obtained on (a) reductive decomposition of $CuAl_4$-LDH and (b) soaking (a) in 6 M NaOH.

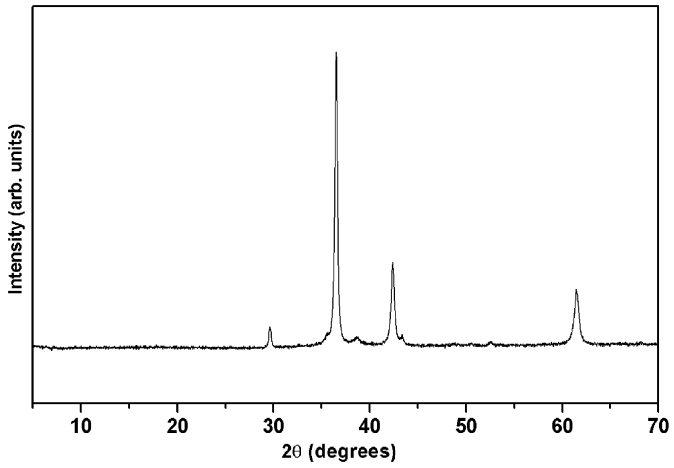

Fig. 11. PXRD pattern of the Cu_2O product obtained on reductive decomposition of Cu_2Al-LDH using ascorbic acid.

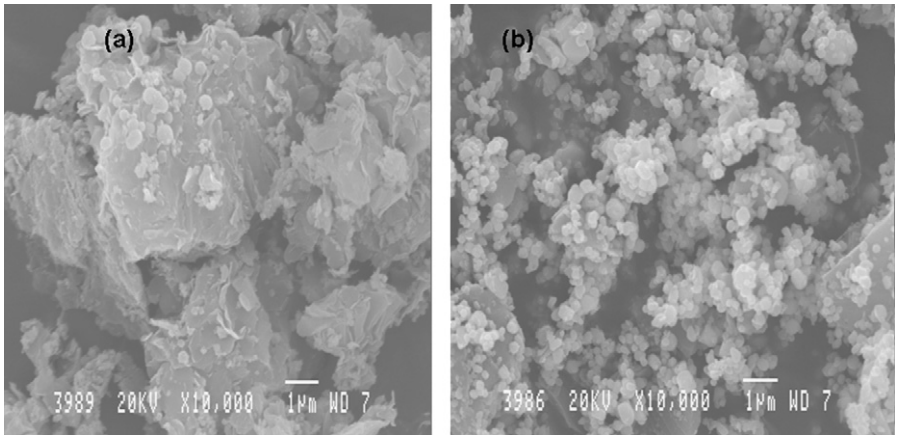

Fig. 10. SEM image of (a) the Cu_2O–$Al(OH)_3$ composite obtained on reductive decomposition of $CuAl_4$-LDH and (b) Cu_2O obtained on leaching of $Al(OH)_3$ from (a).

$\Delta G^0_{298}[Mg(OH)_2] = -199.3$ kcal mol^{-1}, $\Delta G^0_{298}[Co(OH)_2] = -110$ kcal mol^{-1}] [2]. The lower thermal stability of the Cu_2Al-LDH (150 °C) in comparison with other M^{2+}–Al LDHs such as Mg–Al LDH (275 °C) is therefore understandable.

LDHs are generally prepared by coprecipitation at such a pH that the solubility products of both bivalent and trivalent hydroxides are simultaneously exceeded. In general, LDHs may be precipitated over a range of pH values from 7 to10. Johnson and co-workers [19] have shown that for LDHs of the type $M_2Al(OH)_6(CO_3)_{0.5}\cdot H_2O$, the LDH phase is more stable than the divalent hydroxides up to a pH of 10, 9 and 8 for $M =$ Zn, Co and Ni, respectively, and up to a pH of 12 for $M =$ Mg. Further, above the pH range 7–10, the LDH phase is more stable than the related hydroxysalt phases due to the stabilizing influence of the interlayer CO_3^{2-} ion. With the Cu–Al system however, as we have explained earlier, CO_3^{2-} does not confer additional stability to the LDH as it coordinates in C_{2v} mode. Therefore hydrogen bonding interactions which are primarily responsible for the high stability of other M^{2+}–Al–CO_3 LDHs, do not play a significant role in the stability of Cu-Al LDHs. Consequently, the Cu_2Al-LDH precipitates over a much narrower pH range (10–11). At lower pH ranges (7–9) competing hydroxysalt phases (such as malachite) are more stable. At high pH ranges (>11), the amphotericity of $Cu(OH)_2$ causes facile decomposition to CuO. The lower stability of Cu–Al–CO_3 LDHs in solution is also reflected in its lower temperature of decomposition under hydrothermal conditions (150 °C) when compared to other M^{2+}–Al–CO_3 LDHs (180 °C for $M =$ Zn).

It is well known that Cu^{2+} is stabilized by a Jahn-Teller distorted octahedral coordination environment. If the $Cu(OH)_6$ octahedra are only locally distorted, then an average Cu–O bond distance is obtained and the symmetry of the structure as a whole is unaffected. This is the case in the Cu–Cr LDHs where XRD shows that the structure retains rhombohedral symmetry. EXAFS however indicates two Cu–O bond distances (1.97 and 2.31 Å) characteristic of Jahn-Teller distortion [35].

In the Cu–Al LDHs reported here however, it appears that the Jahn-Teller distortion leads to a lowering of the symmetry of the entire structure to monoclinic. It appears that in the Cu–Al LDHs the gain in electronic stability derived from Jahn-Teller distortion around Cu^{2+} is offset by a decrease in lattice energy due to lowered hydrogen bonding interactions of the carbonate anion with the hydroxyl groups of the layer.

All the above factors put together serve to explain the difficulties associated with synthesis of Cu–Al LDHs as well as the lower thermal and aqueous stability of these LDHs in comparison with other M^{2+}–Al–CO_3 LDHs.

In conclusion, Cu–Al LDHs have been prepared by coprecipitation and through an oxide route. While coprecipitation yields a Cu-rich brucite-based LDH, the oxide route yields an Al-rich gibbsite-based LDH. The Cu–Al LDHs have a low thermodynamic stability which facilitates their decomposition by thermal, hydrothermal and reductive routes yielding a bouquet of oxide products with potential for application in different areas.

Acknowledgments

The authors thank the Department of Science and Technology (DST), Government of India (GOI) for financial support. PVK is a recipient of the Ramanna Fellowship of the DST. SB thanks the University Grants Commission, GOI, for the award of a Senior Research Fellowship (NET). Authors thank the Department of Metallurgy, Indian Institute of Science for extending electron microscopy facilities.

References

[1] F. Cavani, F. Trifiro, A. Vaccari, Catal. Today 11 (1991) 173.
[2] H.R. Oswald, R. Asper, Preparation and Crystal Growth of Materials with Layered Structures, D. Reidel Publishing Company, Dordrecht, 1977.
[3] T. Yamaoka, M. Abe, M. Tsuji, Mater. Res. Bull. 24 (1989) 1183.
[4] Y. Lwin, M.A. Yarmo, Z. Yaakob, A.B. Mohamad, W.R. Daud, Mater. Res. Bull. 36 (2001) 193.
[5] R. Trujillano, M.J. Holgado, F. Pigazo, V. Rives, Physica B 373 (2006) 267.
[6] I.Y. Park, K. Kuroda, C. Kato, Solid State Ionics 42 (1990) 197.
[7] A. Alejandre, F. Medina, P. Salagre, X. Correig, J.E. Sueiras, Chem. Mater 11 (1999) 939.
[8] A.M. Fogg, A.J. Freij, G.M. Parkinson, Chem. Mater. 14 (2002) 232.
[9] A.V. Besserguenev, A.M. Fogg, R.J. Francis, S.J. Price, D. O'Hare, V.P. Isupov, B.P. Tolochko, Chem. Mater. 9 (1997) 241.
[10] A.M. Fogg, G.R. Williams, R. Chester, D. O'Hare, J. Mater. Chem. 14 (2004) 2369.
[11] H.C.B. Hansen, C.B. Koch, R.M. Taylor, J. Solid State Chem. 113 (1994) 46.
[12] H. Boehm, J. Steinle, C. Viewager, Angew. Chem. Int. Ed. Eng. 16 (1977) 265.
[13] M. Rajamathi, P.V. Kamath, Bull. Mater. Sci. 23 (2000) 355.
[14] A. Alejandre, F. Medina, X. Rodriguez, P. Salagre, J.E. Sueiras, J. Catal. 311 (1999) 188.
[15] S. Velu, C.S. Swamy, Appl. Catal. A: General 145 (1996) 141.
[16] C. Busetto, G. Del Piero, G. Manara, F. Trifiro, J. Vaccari, J. Catal. 85 (1984) 260.
[17] S. Britto, A.V. Radha, N. Ravishankar, P.V. Kamath, Solid State Sci. 9 (2007) 279.
[18] R.K. Allada, A. Navrotsky, H.T. Berbeco, W.H. Casey, Science 296 (2002) 721.
[19] C.A. Johnson, F.P. Glasser, Clays Clay Miner. 51 (2003) 1.
[20] Vogel's Textbook of Quantitative Inorganic Analysis, fourth ed., Longman Group Ltd, 1978.
[21] V.A. Drits, A.S. Bookin, Layered Double Hydroxides: Present and Future, in: V. Rives (Ed.), Novo Scientist, New York, 2001, pp. 39–92.
[22] A.V. Radha, C. Shivakumara, P.V. Kamath, Clays Clay Miner. 53 (2005) 521.
[23] G.S. Thomas, M. Rajamathi, P.V. Kamath, Clays Clay Miner. 52 (2004) 693.
[24] R. Allmann, Acta Cryst. B 24 (1968) 972.
[25] H.F.W. Taylor, Min. Mag. 39 (1973) 377.
[26] A.S. Bookin, V.A. Drits, Clays Clay Miner. 41 (1993) 551.
[27] M. Bellotto, B. Rebours, O. Clause, J. Lynch, J. Phys. Chem. 100 (1996) 8527.
[28] S. Komarneni, N. Kozai, R. Roy, J. Mater. Chem. 8 (1998) 1329.
[29] T. Sato, K. Kato, T. Endo, M. Shimada, React. Solids 2 (1986) 253.
[30] F. Kooli, C. Depege, A. Ennaqadi, A. De Roy, J.P. Besse, Clays Clay Miner. 45 (1997) 92.
[31] Y. Cuddenec, A. Lecerf, Solid State Sci. 5 (2003) 1471.
[32] M. Rajamathi, S. Thimmaiah, P.E.D. Morgan, R. Seshadri, J. Mater. Chem. 11 (2001) 2489.
[33] L. Zou, F. Li, X. Xiang, D.G. Evans, X. Duan, Chem. Mater. 18 (2006) 5852.
[34] L. Zou, X. Xiang, J. Fan, F. Li, Chem. Mater. 19 (2007) 6518.
[35] H. Roussel, V. Briois, E. Elkaim, A. de Roy, J.P. Besse, J. Phys. Chem. B 104 (2000) 5915.